An RNA recognition motif-containing protein is required for plastid RNA editing in *Arabidopsis* and maize

Tao Sun[a], Arnaud Germain[a], Ludovic Giloteaux[a], Kamel Hammani[b], Alice Barkan[b], Maureen R. Hanson[a], and Stéphane Bentolila[a,1]

[a]Department of Molecular Biology and Genetics, Cornell University, Ithaca, NY 14853; and [b]Institute of Molecular Biology, University of Oregon, Eugene, OR 97403

Edited by Sabeeha S. Merchant, University of California, Los Angeles, CA, and approved February 5, 2013 (received for review November 19, 2012)

Plant RNA editing modifies cytidines (C) to uridines (U) at specific sites in the transcripts of both mitochondria and plastids. Specific targeting of particular Cs is achieved by pentatricopeptide proteins that recognize *cis* elements upstream of the C that is edited. Members of the RNA-editing factor interacting protein (RIP) family in *Arabidopsis* have recently been shown to be essential components of the plant editosome. We have identified a gene that contains a pair of truncated RIP domains (RIP-RIP). Unlike any previously described RIP family member, the encoded protein carries an RNA recognition motif (RRM) at its C terminus and has therefore been named Organelle RRM protein 1 (ORRM1). ORRM1 is an essential plastid editing factor; in *Arabidopsis* and maize mutants, RNA editing is impaired at particular sites, with an almost complete loss of editing for 12 sites in *Arabidopsis* and 9 sites in maize. Transfection of *Arabidopsis orrm1* mutant protoplasts with constructs encoding a region encompassing the RIP-RIP domain or a region spanning the RRM domain of ORRM1 demonstrated that the RRM domain is sufficient for the editing function of ORRM1 in vitro. According to a yeast two-hybrid assay, ORRM1 interacts selectively with pentatricopeptide transfactors via its RIP-RIP domain. Phylogenetic analysis reveals that the RRM in ORRM1 clusters with a clade of RRM proteins that are targeted to organelles. Taken together, these results suggest that other members of the ORRM family may likewise function in RNA editing.

The nucleotide sequences of RNAs are altered co- or post-transcriptionally through RNA editing, a form of RNA processing that differs from capping, splicing or 3′ end formation. First discovered in the mitochondrial RNAs of kinetoplastid protozoa, this phenomenon has been observed in a wide range of organisms and can affect the mRNAs, tRNAs, and rRNAs present in all cellular compartments (reviewed in ref. 1). Nucleotides can be inserted, deleted, or modified through RNA editing. In flowering plants, RNA editing is restricted to organelle transcripts and modifies specific cytidines (C) to uridine (U). The reverse editing reaction, U to C, is also found in a few plant lineages. In *Arabidopsis*, 34 plastid Cs and over 500 mitochondrial Cs have been reported to be edited (2–4). The current consensus view is that RNA editing corrects at the posttranscriptional level mutations that have occurred in plant organelle genomes (5). The absence of editing in some mutants leads to the production of improper proteins that can result in seedling lethality (6).

Despite the discovery of plant RNA editing more than 20 y ago (7–9), only some of the components of the plant editosome are known. *Cis*-elements needed for recognition of C targets are usually found within 30 nt of the C to be edited (10–13). Recognition of the *cis*-elements is performed by members of the PLS subclass of the large pentatricopeptide repeat (PPR)-containing family of proteins (14). However, the enzyme catalyzing the editing reaction, presumably by deamination, is still unknown, although suspicion has fallen on the DYW domain present in some PPR proteins because it contains residues similar to the conserved cytidine deaminase motif (15). The elusiveness of the enzyme responsible for plant RNA editing (16–18) suggests that some important components of the editing machinery are still to be identified.

Recently, members of the RNA-editing interacting protein (RIP) family in *Arabidopsis* have been discovered to be *trans*-factors essential for editing. We identified *Arabidopsis* dual-targeted protein RIP1, an essential plant-editing factor that is required for the editing of numerous Cs both in plastids and mitochondria (19). A *rip1* mutant plant exhibited reduced editing efficiency at 266 mitochondrial C targets, with a major loss of editing for 108. RIP1 is a member of a small protein family that contains 10 members. Other members of the RIP family have also been shown to be required for organelle editing (20). RIP proteins are able to interact selectively with PPR *trans*-actors and also with each other (19, 20); however, their function in the plant editosome remains unclear.

Here we report the identification of a unique protein that is both a member of the RIP family and the RNA recognition motif (RRM)-containing family. This protein carries an RRM at its C terminus, unlike any other RIP domain-containing proteins. The RRM is the most widespread motif involved in RNA binding and is found in all kingdoms (21). However, the RRM domain of this unique protein is most similar to the domain present in an identifiable clade of RRM proteins, most of which are either known to be localized or are predicted to be targeted to plant organelles. We therefore refer to this RRM subfamily as the organellar RRM (ORRM) family. As the founding member of the family, At3g20930 has been named ORRM1. Identification of ORRM1 as an editing factor implicates a previously undescribed class of RRM-containing proteins as potentially

Significance

Transcripts in plant organelles are altered by conversion of cytidines to uridines in a process termed RNA editing. Members of two protein families have been identified in the plant editosome, but its complete composition is unknown. Now a unique protein that contains an RNA recognition motif has been found to be essential for editing of multiple plastid transcripts in both *Arabidopsis* and maize. Phylogenetic analysis indicates that this protein belongs to a sub-family of RNA recognition-motif proteins predominantly predicted to be targeted to organelles and that are thus likely to play roles in organelle RNA metabolism.

Author contributions: T.S., A.B., M.R.H., and S.B. designed research; T.S., A.G., K.H., and S.B. performed research; T.S. contributed new reagents/analytic tools; T.S., A.G., L.G., A.B., M.R.H., and S.B. analyzed data; and A.B., M.R.H., and S.B. wrote the paper.

The authors declare no conflict of interest.

This article is a PNAS Direct Submission.

[1]To whom correspondence should be addressed. E-mail: sb46@cornell.edu.

This article contains supporting information online at www.pnas.org/lookup/suppl/doi:10.1073/pnas.1220162110/-/DCSupplemental.

involved in RNA editing, as well as other aspects of organelle RNA metabolism.

Results

Identification of a Protein Carrying Truncated RIP Domains. A blastp search for homologs to the RIP1 protein returned the 10 previously reported members of the RIP family (19, 20) as well as a unique RIP family member, encoded by the gene At3g20930 (Fig. 1*A*). This protein was not previously described as either a RIP or MORF protein (19, 20). We used the MEME software (22) to identify four highly significant motifs in the RIP family (Fig. 1*B*). The RIP block can be defined by the following series: motif 1-gap-motif 2-motif 3-motif 4 (Fig. 1*A*). The distal motif 4 found in RIP7 is below the threshold of e-10 (*P* value = 9.6 e-6). Most RIP proteins possess a complete RIP block (Fig. 1*C*). The unique member of the RIP family encoded by At3g20930 exhibits a duplication of truncated RIP blocks; the first block, from amino acid 89 to amino acid 147, contains a degenerate motif 1 plus motifs 2 and 3, and the second RIP block from amino acid 163 to amino acid 250 contains motifs 1–3. Both RIP blocks in At3g20930 lack motif 4 (Fig. 1*C*).

At3g20930 Protein Contains an RNA Recognition Motif at Its C Terminus and Belongs to a Clade of RRM Proteins. A motif search with Motif Scan (http://myhits.isb-sib.ch/cgi-bin/motif_scan) identified the presence of a RRM at the C terminus of the protein. The RRM domain is ~80-aa long and contains two short consensus sequences, RNP1 (octamer) and RNP2 (hexamer), which are characteristic of RRMs (Fig. 2*A*).

In *Arabidopsis*, 196 RRM-containing proteins were previously identified through an in silico search for the RRM motif (23). A blast search using the RRM domain of the protein encoded by At3g20930 revealed that this domain was more closely related to the RRM found in two distinct families described by Lorkovic and Barta (23), the glycine-rich RNA-binding proteins (GR-RBP) and the small RNA-binding proteins (S-RBP). A common feature of these two protein families is their similar domain organization with one N-terminal RRM and a C-terminal extension. GR-RBPs are represented by eight members, but 15 proteins were annotated as S-RBP (23). At the time of the Lorkovic and Barta's (23) report, Vermel et al. (24) identified by biochemical means a family of mitochondrial-specific RRM-containing proteins that they named mitochondrial RNA-binding proteins (mRBP). The 11 mRBPs belong to either the GR-RBP or the S-RBP family. Fig. 2*A* illustrates the strong similarity between the RRM domains found in the At3g20930 product, the GR-RBPs, and the mRBPs. To verify the similarity between the RRM domains found in the At3g20930-encoded product, the GR-RBPs, and the mRBPs, we aligned them with the RRM of a protein encoded by At5g46840, which does not belong to any of these subfamilies (Fig. 2*A*).

When we used the MEME software with the number of motifs set at 4, and width greater than 5 but less than 20 amino acids, four motifs were identified in this set of RRMs that can define the unique subfamily related to the RRM present in the protein

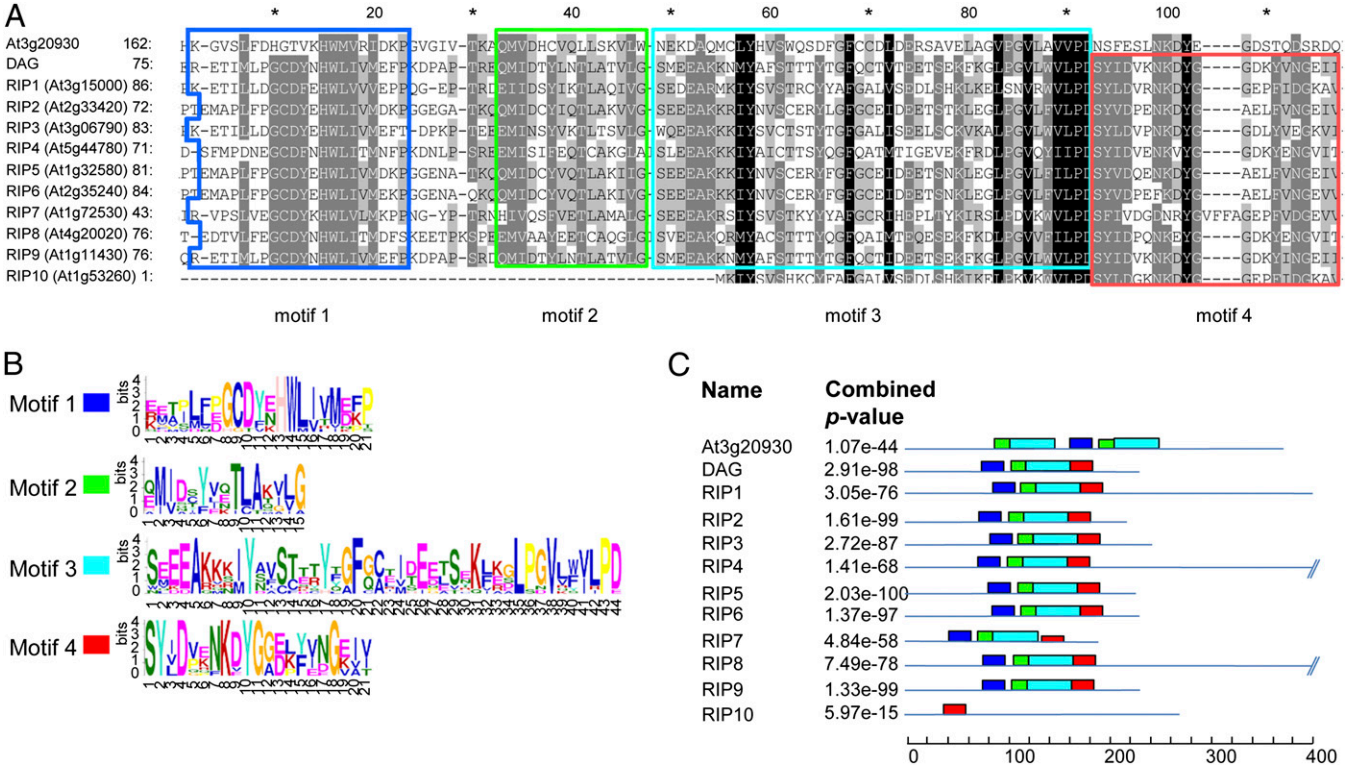

Fig. 1. The protein encoded by At3g20930 belongs to the RIP family and contains a pair of truncated RIP domains. (*A*) Alignment of the conserved regions in the *Arabidopsis* RIP proteins (RIP1 to RIP10), the DAG protein from *Antirrhinum majus* (GenBank CAA65064), and the protein encoded by At3g20930 was performed using T-Coffee Version_9.03, and displayed using GeneDoc with the conserved residue shading mode and similarity groups enabled. Overlaid on the aligned sequences are the four motifs detected by the MEME software version_4.9.0. (*B*) The RIP domain contains four motifs uncovered by MEME. The settings were 6 aa < width < 100 aa, maximum number of motifs to find was four. All four motifs are highly significant (E-values: 7.8e-208, 5.5e-111, 3.7e-86, 4.2e-52). Each motif is given its sequence logo showing the likelihood of residue at each position. (*C*) The combined motif diagrams are shown for each of the RIP protein, the DAG protein, and the protein encoded by At3g20930. The height of a motif is truncated when its *P* value is > 1e-10, for example, motif 3 for RIP7.

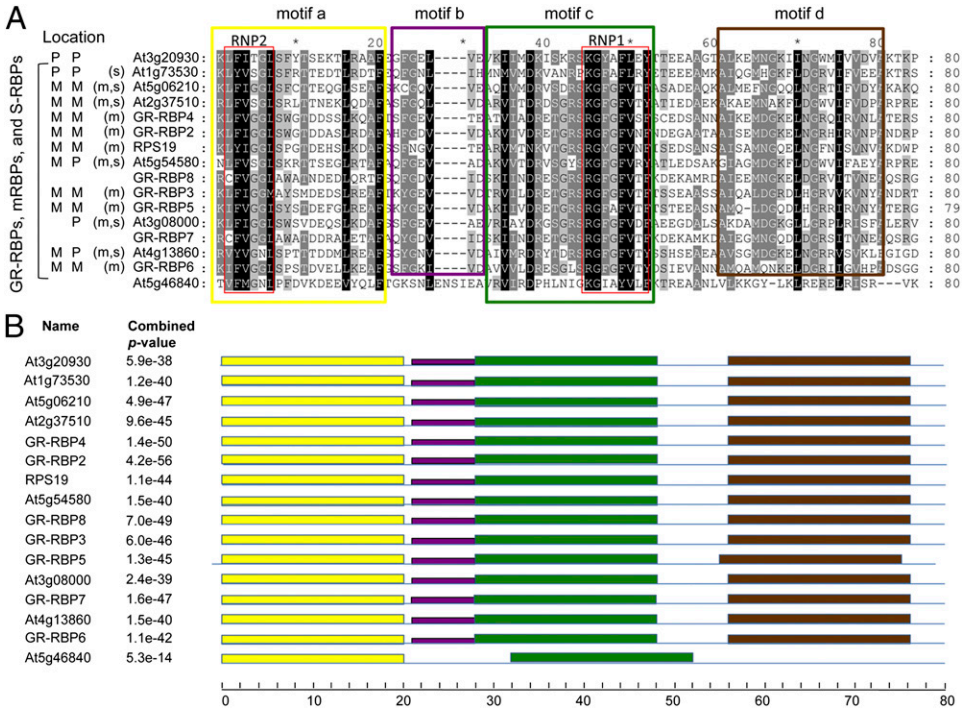

Fig. 2. The RRM domain found at the C terminus of ORRM1 shows most similarity to the RRMs from glycine-rich (GR), mitochondrial (m), and small (S), RBPs. (*A*) RRMs from the protein encoded by At3g20930, the GR-RBPs, the mRBPs, and the S-RBPs were aligned by T-Coffee version_9.03, and displayed using GeneDoc with the conserved residue shading mode and similarity groups enabled. Depending on the database of protein domains searched, prosite or pfam, the RRM motif was located at position 282–360 with a E-value of 1.3e-11, or at position 284–350 with an E-value of 2.2e-24, respectively. Overlaid on the aligned sequences are the four motifs detected by the MEME software version_4.9.0. Location on the left of each protein refers to the subcellular location predicted by Predotar or TargetP, P, plastid; M, mitochondrion. In parenthesis preceding the name of the protein is given the annotation (m) mitochondrial (24) or (s) small (23). (*B*) Combined *P* values and block motifs computed by the MEME software indicated that the RRMs fromORRM1, the GR-RBPs, the mRBPs, and the S-RBPs belong to the same family defined by motifs a, b, c, and d. The product encoded by At5g46480, a RRM-containing protein (motifs a and c only) does not belong to this family.

containing two RIP motifs. Two of the four motifs, motif "a" and motif "c," are found in the RRM domains of the unique subfamily but also in the RRM domain of the protein encoded by At5g46840 (Fig. 2*B*). In contrast, motif "b" and motif "d" are specific to the RRM domains found in the product encoded by the RIP-family protein At3g20930, as well as in the GR-RBPs and the mRBPs (Fig. 2*B*). All of the proteins shown in Fig. 2*A* are predicted to be located in plastids or mitochondria. We have therefore named the group of organelle-targeted proteins containing the four motifs described in Fig. 2 the ORRM family. The protein encoded by At3g20930 is hereafter designated as ORRM1.

A Pfam domain search using At3g20930 (ORRM1) as a query identified 642 RRM containing regions in the *Arabidopsis thaliana* genome. As examples, putative RNA-binding proteins, poly (A)-binding ribonucleoproteins, splicing-factors, U2 small nuclear ribonucleoproteins, *Arabidopsis-mei2-like* proteins, and chloroplast ribonucleoproteins were retrieved. Several clearly identifiable clusters in the phylogenetic tree can be distinguished, suggesting that RRMs can be classified according to groups of proteins of the same function, such as U2 small nuclear ribonucleoproteins, poly(A)-binding proteins, splicing factors, and chloroplast RNA-binding proteins (CP) (Fig. 3).

ORRM1 appears to form a monophyletic group with members of the glycine-rich RNA binding proteins (Fig. 3). The topology of the tree constructed by the unweighted pair-group method using arithmetic averages (UPGMA), maximum-pasimony, maximum-likelihood, and minimum-evolution methods was not different from that of the Neighbor-Joining tree presented here, supporting a consistent grouping of the proteins.

T-DNA Insertional Mutant in *ORRM1* Exhibits Severe Defects in Plastid Editing. We obtained an *Arabidopsis* mutant from the *Arabidopsis* Biological Resource Center stock collection and verified that it was homozygous for a T-DNA insertion in the first exon of *ORRM1* (Fig. 4*A*) (SALK_072648, designated here as *orrm1*). The homozygous mutant did not show any phenotypic defect when grown under growth room conditions (Fig. 4*B*). No expression of *orrm1* was detected by RT-PCR (Fig. 4*C*). We examined the organelle transcriptome of the mutant for editing defects because other proteins carrying RIP domains have been shown to be editing factors (19, 20). We analyzed the plastid RNA editing extent with a new methodology based on RNA-seq. Briefly, total RNA is isolated from leaves and RT-PCR products corresponding to known organelle genes are obtained by using gene-specific primers. The products are mixed in equimolar ratio, sheared, and used as templates to produce an Illumina TruSeq library. This RNA-seq analysis demonstrated that ORRM1 is a plastid editing factor; 12 among 34 plastid sites exhibit a severe reduction of editing extent in the mutant relative to the wild-type (Fig. 4*D*).

In addition to the 12 sites where editing is reduced by 90% or more, 9 plastid sites exhibit a reduction of editing extent between 10 and 90% in the mutant. Thus, 62% (21 of 34) of the plastid-editing sites are under the control of ORRM1 (Table S1). We confirmed the gene-specific RT-PCR results on the *orrm1* mutant by performing RNA-seq on total plastid RNA. For this purpose, total RNA was extracted from chloroplasts purified from mutant and the wild-type and reverse-transcribed using random hexamers. The number of reads per chloroplast gene ranged from ~20 to ~5,000 (Table S1). The numbers of reads are much higher in the gene-specific RT-PCR– generated Illumina library, with averages of ~7,000 and ~11,000 for the wild-type and the mutant, respectively (Table S1). Despite the difference in depth coverage between the gene-specific and total plastid RNA Illumina libraries, the reductions of editing extent in the mutant are highly consistent between the two assays (Fig. S1 and Table S1).

To verify the suitability of the RNA-seq method for assaying RNA editing, we performed poisoned primer extension (PPE) on a selection of transcripts and compared the results to the gene-specific RNA-seq and total plastid RNA-seq data (Fig. 5). In the PPE assay, cDNA serves as a template for an extension reaction in the presence of a dideoxy G. When dideoxy G is incorporated, the extension stops at the first unedited C that is encountered by the enzyme. The products of edited vs. unedited transcripts will differ in size; the amount of each product can be

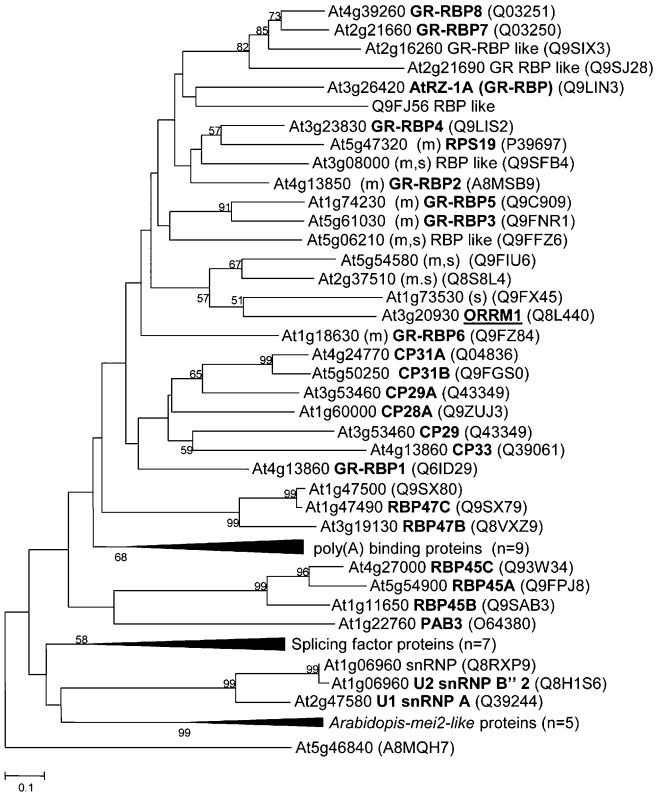

Fig. 3. Phylogenetic tree based on the amino acid sequences of the RRM motifs in RRM-containing proteins (84 amino acids considered). The tree was inferred using the Neighbor-Joining method, and evolutionary distances were computed using the Poisson-correction method. The scale bar corresponds to 0.1 substitutions per site. CP, chloroplast ribonucleoprotein; PABP, poly(A) binding protein; snRP, small nuclear ribonucleoprotein. In the ORRM1 clade, the figure in parenthesis is the annotation (s) for small given in Lorkovic and Barta (23), or (m) for mitochondrial given in Vermel et al. (24).

accurately monitored on gels. As an example, we show the PPE data for three C targets of editing in the *ndhD* transcript, one has an editing extent that is unaffected by the *orrm1* mutation (Fig. 5*A*), but the other two exhibit almost complete loss of editing (Fig. 5 *B* and *C*). We performed PPE assays on six additional transcripts (Fig. S2) and demonstrate the consistency of the two assays by graphing the RNA-seq editing extent data against the data from the PPE assay (Fig. 5*D*).

We also surveyed the mitochondrial transcriptome of the *orrm1* mutant with gene-specific primers; none of the 574 mitochondrial sites assayed showed a significant difference in editing extent between the mutant and the wild-type. Thus, ORRM1 is an editing factor that is specific to plastids.

RNA Editing Defects Are Detected in *orrm1* Chloroplast Transcripts That Do Not Differ in Abundance from Wild-Type Transcripts. Although our gene-specific RNA-seq method does not provide any information on transcript abundance, our RNA-seq experiments using total chloroplast RNA do allow us to quantify relative abundance of transcripts from different genes. The number of total plastid RNA reads corresponding to each plastid transcript in the *orrm1* and wild-type total plastid RNA data exhibit little variation (Table S1), indicating that changes in RNA abundance do not explain the effect of the mutation on editing at specific C targets. To verify that abundance of transcripts carrying Cs affected in editing extent do not vary greatly between the mutant and wild-type, we performed RNA blots with total chloroplast RNA from *orrm1* and wild-type plants (Fig. S3). We used three probes corresponding to the *matK*, *ndhB*, and *ndhD* genes, whose transcripts carry C targets with reduced editing in the *orrm1* mutant. These blots demonstrate that there is no difference in the complexity of the RNA profile or abundance of particular transcript species between wild-type and *orrm1* (Fig. S3). In addition, different Cs located on the same transcript sometimes vary greatly in their editing extent in the *orrm1* mutant. Both *ndhB* and *ndhD* carry a C target that is unaffected in the *orrm1* mutant, but the other Cs in the *ndhB* and *ndhD* exhibit major reduction in editing efficiency in the mutant (Fig. 5 and Fig S2).

RRM Domain Can Rescue the Editing Defect in *orrm1* Protoplasts. We determined whether the T-DNA insertional mutation could be complemented by transient expression of *ORRM1* under the control of a 35S promoter in mutant protoplasts. PPE assay demonstrated that mutant protoplasts transfected with the construct carrying the full-length *ORRM1* exhibited significant increase in editing extent (Fig. 6*A*, lane F). The extent of editing for *ndhB*-872 and *rps12*-i58 in transfected mutant protoplasts, 43% and 27% respectively, is sufficient to observe a very distinct edited product band on the PPE gel compared with untransfected protoplasts (Fig. 6*A*, lane NT). As expected in a transient expression assay, the level of editing extent of *ndhB*-872 and *rps12*-i58 in the transfected protoplasts does not reach the level observed in the wild-type plant, which is 95% and 40%, respectively (Table S1). Seventy-six percent (16 of 21) of the plastid sites assayed that

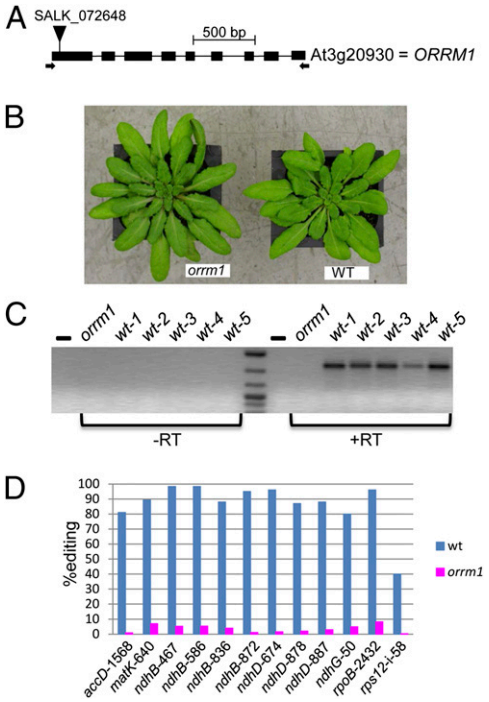

Fig. 4. A T-DNA insertional mutant in *ORRM1* is severely impaired in plastid editing. (*A*) Schematic representation of the model gene for *ORRM1* with exons represented as squares and introns as lines, the T-DNA insertion is shown as a triangle in the first exon. The primers used for the RT-PCR are indicated by arrows. (*B*) The homozygous mutant plant (*Left*) does not show any phenotypic defect compared with a Columbia wild-type plant (*Right*) when grown under growth-room conditions. (*C*) No expression of ORRM1 is detectable by RT-PCR after 45 cycles in the *orrm1* mutant, although expression is readily observed in wild-type. (*D*) Thirteen plastid sites show a severe reduction of editing extent (Δ*ORRM1*) > 90% in the *ORRM1* T-DNA insertional mutant. Because the *orrm1* homozygous mutant line was in a Columbia background, five wild-type siblings of other *rip* family insertional mutants that were in a Columbia background served as positive controls.

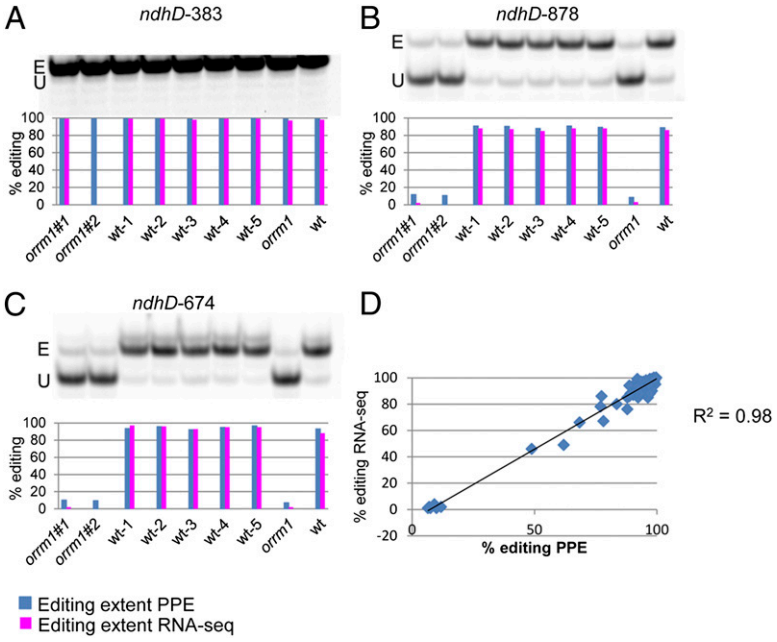

Fig. 5. PPE assay validates the editing extents derived from RNA-seq. (*A–C*) Acrylamide gels separate the PPE products obtained from samples used in this study. E, edited; U, unedited. The name of the site assayed is given above each gel. The quantification of editing extent derived from the measure of the band's intensity is represented by a bar below each lane of the acrylamide gels (blue diagonal background). By way of comparison, the editing extent derived from RNA-seq is represented by a magenta bar. RNA-seq was performed on gene specific cDNAs for *orrm1#1*, wt-1, wt-2, wt-3, wt-4, and wt-5, and on total plastid RNA for *orrm1* and wt. *orrm1#2* was not analyzed by RNA-seq. (*D*) The correlation between the editing extent values derived from PPE assay and RNA-seq verifies RNA-seq is a sound method to determine editing extent. The correlation was calculated by plotting 72 points (8 samples × 9 PPE gels).

showed a reduction or a lack of editing extent in the mutant exhibited a significant increase of their editing extent in the transfected protoplasts with the full-length *ORRM1* (Fig. 6*B*).

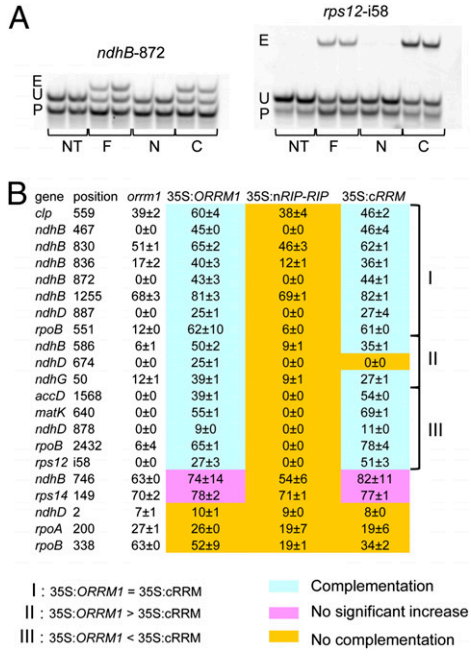

Fig. 6. ORRM1 is able to complement *orrm1* protoplasts with its RRM domain, not its RIP domain. (*A*) PPE products from not transfected protoplasts (NT), protoplasts transfected with a construct encoding a full-length (F), the N-terminal portion (N) that contains the RIP-RIP domain, or the C-terminal portion (C) that contains the RRM domain. Above each gel is given the name of the editing site (gene-position), E, edited; U, unedited; P, primer. The presence of the edited bands is only observed in protoplasts transfected with the full-length construct or with a construct encoding the RRM. (*B*) Twenty-three plastid sites showing a decrease in the *orrm1* mutant were assayed for complementation in the transfected mutant protoplasts. Among the 16 sites complemented by the full-length construct, 15 also exhibit a complementation by the construct encoding the RRM domain of ORRM1.

Similar transfection experiments were performed with constructs encoding either the N-terminal portion of ORRM1 that contains the duplicated RIP-RIP region (Fig. 6*A*, lane N) or the C-terminal portion, which carries the RRM domain (Fig. 6*A*, lane C). Of the two truncated constructs tested, only the construct encoding the RRM domain was able to complement the editing defect of the mutant (Fig. 6*A*, lane C). Among the 16 sites partially complemented by the full-length *ORRM1*, 15 showed a significant increase of editing extent in the mutant protoplasts upon transfection with the construct encoding the RRM domain (Fig. 6*B*). At three sites, the full-length construct was able to complement the editing defect more efficiently than did the RRM construct. Among these sites, *ndhD*-674 is the only one for which no effect of the RRM construct was observed (Fig. 6*B*). The RRM construct more efficiently complemented five sites than did the full-length construct; among these sites, *rps12*-i58 shows almost twice the amount of edited transcripts in protoplasts transfected with the RRM construct than with the full-length construct (Fig. 6*A*). The increase of editing extent in transfected protoplasts was below the significance threshold for two sites, *ndhB*-746 and *rps14*-149. An absence of effect from the transfection with either the full-length or the RRM construct was observed in only three of the assayed sites (Fig. 6*B*).

Maize ORRM1 Ortholog Is Required for the Editing of Both Orthologous and Maize-Specific Sites. Maize mutants with *Mu* transposon insertions in the ortholog of ORRM1 (Zm-*orrm1*) were recovered during the identification of causal mutations in a large collection of nonphotosynthetic mutants (http://pml.uoregon.edu/photosyntheticml.html). The Zm-*orrm1* mutants originally came to our attention because of their unusual spectrum of protein deficiencies (see below), which could not easily be explained by defects in known chloroplast biogenesis genes. Therefore, the mutants were selected for gene identification with a high-throughput method for sequencing *Mu* insertion sites (25) (*Materials and Methods*). Two alleles were identified, both with an insertion in the first exon (Fig. 7*A*). Complementation crosses yielded heteroallelic mutant progeny (Zm-*orrm1-1*/Zm-*orrm1-2*) displaying a pale green phenotype (Fig. 7*B*). The mutant progeny of complementation crosses were used for the molecular analyses summarized below, as phenotypes expressed in this material must

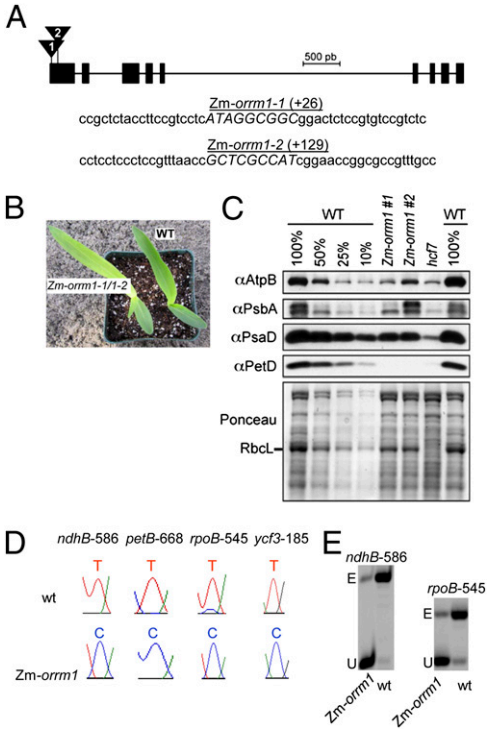

Fig. 7. The maize orthologous gene to *ORRM1* encodes a plastid editing factor. (*A*) Gene model of Zm-*ORRM1* with exons (squares) and introns (lines). The two independent *Mu* insertions are shown as triangles in the first exon, with the 9-bp target-site duplication shown in capital letters. The insertions in exon 1 are at the indicated position with respect to the start codon. (*B*) Zm-*orrm1-1/1–2* complementation cross progeny mutant plant is a photosynthetic mutant exhibiting a pale green phenotype (*Left*) compared with the wild-type (*Right*). (*C*) Immunoblot analysis of photosynthetic enzyme accumulation in *Zm-orrm1-1/Zm-orrm1-2* mutants. An immunoblot of total leaf extracts (5 μg or the indicated dilutions) was probed with antibodies to the indicated proteins. The same blot stained with Ponceau S is shown below; the band corresponding to the large subunit of Rubisco (RbcL) is marked. The Zm-*orrm1* mutants are siblings derived from the same complementation cross (genotype Zm-*orrm1-1*/Zm-*orrm1-2*). *hcf7* is a previously described mutant with a global decrease in chloroplast translation (65). (*D*) Bulk-sequencing electrophoretograms of RT-PCR products from *Zmorrm1* and a wild-type sibling at four plastid sites show a total loss of editing in Zm-*orrm1* as no edited peak (T) is detectable. (*E*) PPE assay reveals a residual editing extent in Zm-*orrm1* mutant plant for *ndhB*-586 and *rpoB*-545, 7% and 14%, respectively.

result from disruption of the Zm-*orrm1* gene. These heteroallelic mutants will be referred to hereafter as Zm-*orrm1* mutants.

Defects in the major photosynthetic enzyme complexes were profiled in Zm-*orrm1* mutants by quantifying one core subunit of each complex: PetD of the cytochrome b_6f complex, PsaD of photosystem I, PsbA of photosystem II, RbcL of Rubisco, and AtpB of the plastid ATP synthase (Fig. 7*C*). The accumulation of these proteins is known to parallel that of other closely associated subunits in the same complex. Zm-*orrm1* mutants have a severe deficiency for PetD (<<10% of normal levels), a moderate deficiency for PsaD (roughly 25% of normal levels), and mild, somewhat variable reductions in RbcL, AtpB, and PsbA (40–80% of normal levels). In light of the editing defects observed in *Arabidopsis orrm1* mutants, a reasonable hypothesis was that these protein deficiencies result from defects in chloroplast RNA editing.

Indeed, when all 27 known edited nucleotides in maize chloroplasts were assayed by bulk sequencing of RT-PCR products, multiple RNA editing defects were detected in the Zm-*orrm1* mutant (Fig. S4). Four sites, *ndhB*-586, *petB*-668, *rpoB*-545, and *ycf3*-185 exhibited a complete loss of editing (Fig. 7*D*). Only five plastid sites did not show any reduction of editing extent in the Zm-*orrm1* mutant (Fig. S4 and Table S2). Maize and *Arabidopsis* plastid transcripts share seven common editing sites so we more precisely assayed the editing extent of these sites in the Zm-*orrm1* mutant by a PPE assay using fluorescent primers designed for *Arabidopsis* (Fig. 7*E* and Fig S5). The PPE assay is more sensitive than the bulk-sequencing assay, and indicates residual editing of the *ndhB*-586 and *rpoB*-545 sites in the maize mutant (Fig. 7*E*).

These RNA editing defects correlate well with the protein deficiencies in Zm-*orrm1* mutants. The failure to edit *petB*-668 could account for the severe PetD deficiency, as this editing event is essential for the accumulation of the cytochrome b_6f complex (26). The reduction in *ycf3*-185 and *ycf3*-44 editing is likely to account for the loss of PsaD, as Ycf3 is required for the assembly and accumulation of photosystem I (27, 28). The minor loss of other proteins likely results from compromised chloroplast transcription and translation, possibly because of defects in the editing of *rpoB*, *rpl20*, and *rps8* (encoding subunits of the plastid RNA polymerase, large ribosomal subunit, and small ribosomal subunit, respectively).

The maize and *Arabidopsis* orthologous *ORRM1* genes evidently play similar roles in editing of the C targets that are shared between the two species. Sites such as *ndhB*-586 exhibit a pronounced reduction of editing extent in both *Arabidopsis* and maize mutants (Tables S1 and S2). In contrast, the editing extents of *ndhB*-1481 and *rps14*-80 exhibit little or no change in either the *Arabidopsis* or maize mutants (Tables S1 and S2).

The similarity in editing function between the maize and *Arabidopsis* orthologs was further analyzed by transfecting *Arabidopsis* mutant protoplasts with the Zm-*ORRM1* under the control of either the 35S or the CMV immediate-early promoter. The CMV promoter is used in mammalian expression systems; however, apparently it is able to drive the expression of Zm-*ORRM1* in *Arabidopsis* protoplasts (Fig. S6*A*). Unexpectedly, the editing extent of six plastid sites was significantly higher in mutant protoplasts transfected with the CMV construct than with the 35S promoter-containing construct (Fig. S6*A*). In fact, the editing of *rpoA*-200 was partially complemented by the CMV maize construct but not with the 35S construct carrying the maize gene (Fig. S6*A*). Expression of *Zm-ORRM1* from the CMV promoter may be higher than the 35S promoter in these experiments. The majority of the plastid sites experienced a significant increase of editing extent in transfected mutant protoplasts independently of the promoter used in the construct (Fig. S6*A*).

Taken together, the similarity in the editing defects in the maize and *Arabidopsis* mutants and the transfection experiments with the Zm-*ORRM1* strongly support a similar function in editing for the maize and *Arabidopsis* genes. The maize and *Arabidopsis* RRM domains are highly conserved (Fig. S6*B*), which likely explains the cross-species complementation of function.

Recombinant At-ORRM1 Binds Near Several ORRM1-Dependent Editing Sites in Vitro. ORRM1 includes an RRM domain and so was anticipated to be an RNA-binding protein. However, ORRM1 could potentially act in one of two ways: (*i*) it could bind RNA nonspecifically, relying on recruitment to specific editing sites by interaction with a PPR specificity factor; or (*ii*) it could contribute to editing site choice by binding with specificity near its targets. To address these alternatives, we performed RNA binding assays with purified recombinant ORRM1 fused to maltose binding protein (MBP-ORRM1) (*Materials and Methods*). Gel mobility-shift assays were used to monitor binding to synthetic RNAs mapping between −40 and +19 with respect to the ORRM1-dependent editing sites *ndhD*-674, *accD*-1568, and *matK*-640. Two sequences lacking editing sites were used as negative controls: a 60-mer spanning the *Arabidopsis petB* 5′ UTR

and a 50-mer from the *psbH* 5′ UTR. MBP-ORRM1 consistently bound with much higher affinity to the *ndhD* RNA than to the negative controls (Fig. 8 and Fig. S7). MBP-ORRM1 also bound preferentially to the *accD* RNA in comparison with the *petB* negative control, albeit with lower affinity than it bound to the *ndhD* RNA. However, MBP-ORRM1 exhibited only minimal preference for the *matK* RNA under the binding conditions explored. The boundaries of the *cis*-element required to specify *matK*-640 editing is not known, so it remains possible that ORRM1 interacts specifically with RNA outside the assayed region. Taken together, these results support the view that ORRM1 has intrinsic specificity for sequences near at least some of its RNA targets.

ORRM1 Interacts with an Editing Recognition *trans*-Factor Through its Duplicated RIP Moiety. We have previously shown that RIP1 interacts via its RIP moiety with RARE1, a PPR-DYW *trans*-factor that controls the editing of the plastid editing site *accD*-794 (19). A yeast two-hybrid (Y2H) test was performed between ORRM1 and a series of PPR-PLS *trans*-factors known to control the editing extent of plastid sites. We chose the PPR-PLS motif-containing proteins to be tested based on the effect of the *ORRM1* mutation on the editing extent of the sites they control. CRR28 is required for the editing of *ndhB*-467 and *ndhD*-878 (16) and OTP82 is needed for editing of *ndhG*-50 and *ndhB*-836 (17). The editing extent of these sites is severely reduced to more than 90% in the *orrm1* mutant (Table S1). In the Y2H analysis we also included RARE1 and OTP84, which are required for the editing of *accD*-794, *ndhF*-290, *ndhB*-1481, and *psbZ*-50, respectively (29, 30). The editing extent of *accD*-794, *ndhF*-290, *ndhB*-1481, and *psbZ*-50 in the *orrm1* mutant is identical to the wild-type plant (Table S1).

CRR28 and OTP82 interacted with ORRM1 in the Y2H assay, whereas RARE1 and OTP84 did not (Fig. 9*A*). The lack of interaction between ORRM1 and the latter two PPR-PLS editing *trans* factors is expected given the absence in the *orrm1* mutant of an effect on the editing extent of the sites they control (Fig. 9*A* and Table S1). By testing constructs with either the RIP or the RRM region of ORRM1, we determined that the RIP region is sufficient to interact with CRR28 and OTP82, whereas the RRM domain is not (Fig. 9*B*).

Discussion

We report here the identification and characterization of ORRM1, a unique editing factor that controls the editing extent

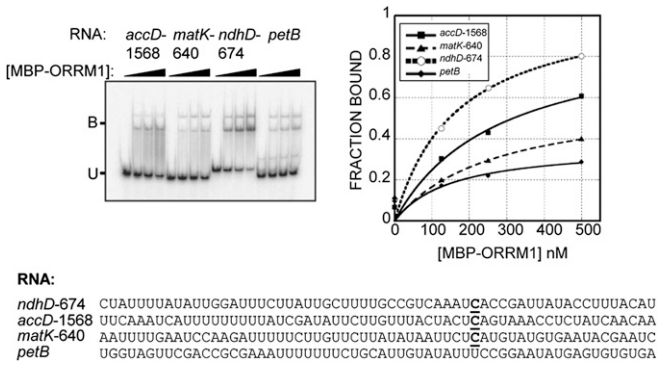

Fig. 8. RNA binding activity of recombinant ORRM1. Gel mobility-shift assays were performed with MBP-ORRM1 at the indicated concentrations, together with the radiolabeled RNAs shown below (edited site underlined). The *petB* sequence is not edited and serves as a negative control. MBP has been shown to lack RNA binding activity under the conditions used here (66). B, bound RNA; U, unbound RNA.

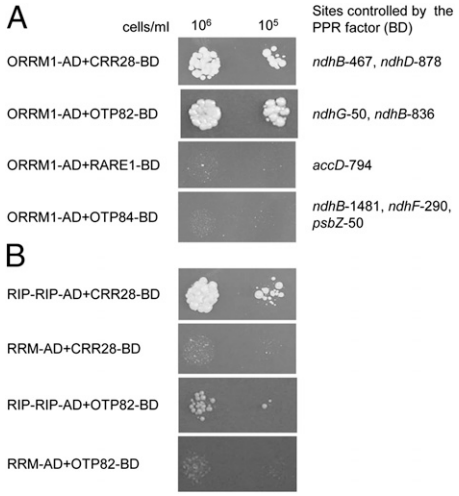

Fig. 9. ORRM1 interacts selectively with PPR-PLS recognition *trans*-factors via its RIP domain in a Y2H assay. (*A*) Yeast colonies were able to grow in selective media (-histidine) only when ORRM1 fused to the AD and CRR28 or OTP82 fused to the BD were coexpressed into transformed yeast. (*B*) The interaction between ORRM1 and CRR28 or OTP82 is mediated by the RIP domain of ORRM1 as yeast colonies were able to grow in selective media (-histidine) only when the RIP region of ORRM1 fused to the AD and CRR28 or OTP82 fused to the BD were coexpressed into transformed yeast. No yeast growth was observed when the RIP-AD fusion protein was substituted by the RRM-AD fusion protein. The interaction between the RIP domain of ORRM1 and OTP82 (*B*, third panel from the top) is weaker than the interaction of the full lengthORRM1 (*A*, second panel from the top). None of the constructs used in these experiments showed autoactivation for HIS3 reporter.

of 62% of the plastid Cs targeted for editing in *Arabidopsis* and 81% of C targets in maize. We have demonstrated that ORRM1 is a true editing factor because the effect cannot be explained as an indirect effect caused by changes in RNA transcript abundance. Reduced transcript abundance can indirectly affect the level of editing extent, if RNA is degraded before it is edited (31), or if transcript levels increase to levels high enough to saturate the editing machinery (32). We have verified that there is no significant difference in transcript abundance between the wild-type and the *Arabidopsis orrm1* mutant by performing Northern blots that are consistent with the cpRNA-seq data (Table S1). Therefore, RNA editing defects do not correlate with transcript abundance in the mutant. In addition, RNA editing defects in the mutant are site-specific, as demonstrated for transcripts with multiple editing sites, such as *accD*, *ndhD*, and *ndhB*, which exhibit reduced editing extent of some sites but not others on the same transcript (Fig. 5 and Fig. S2).

The current model for the specificity of the C to be edited in plant organelles postulates two elements: a *cis* sequence primarily upstream of the targeted C and a *trans*-factor that recognizes the *cis*-element. The *cis*-acting elements have been delineated to be about 30 nt surrounding the editing site for both organelles (33, 34). Plant site-specific editing factors belong to the PLS subfamily of the PPR protein family (14). Binding of the *cis*-element and the PPR-PLS *trans*-factor has been demonstrated in several instances (35–37). Recent reports have demonstrated that RIPs, another small class of proteins, are also plant organelle editing transfactors (19, 20). Although the molecular function of the RIPs remains unknown, they are essential components of the plant RNA editing machinery; *rip* mutants exhibit severe defects in organelle editing. We have shown that RIP1 functions in an editing complex with RARE1, a plastid PPR-PLS protein, and that it binds RARE1 via its RIP-containing moiety (19). We have demonstrated in this study that the portion of ORRM1 that is similar to the RIP family is able to

bind to PPR-PLS motifs that are found on a *trans*-factor that controls the editing of sites for which ORRM1 is required. The specificity of ORRM1 in the editing of particular sites might thus sometimes be achieved through binding to particular PPR-PLS recognition factors. We have demonstrated that CRR28 can interact directly with ORRM1, but interactions with other PPR proteins might be indirect, mediated through binding to other RIPs, as some RIPs have been shown to interact with each other (20).

ORRM1, unlike true members of the RIP family, possesses a duplicated set of truncated RIP motifs (Fig. 1). This unconventional structure, coupled with the presence of the RRM domain not present in other members of the RIP family, suggests that the gene encoding this protein might have originated through recombination during evolution. There are numerous examples of associations of the RRM with other domains; 21% of the RRMs in eukaryotic proteins are found in association with other domains (21). For example, in *Arabidopsis*, the mitochondrial ribosomal protein RPS19 is nuclear-encoded and carries an N-terminal RRM. The RPS19 protein is thought to have originated from a fusion from a genomic RRM-encoding gene and a mitochondrial *rps19* gene that was transferred to the nucleus (38). A MAST search for sequences in the nonredundant protein database with the *Arabidopsis* RIP motif defined by the MEME software (Fig. 1) returned many proteins; however, the ones carrying the twin truncated RIP domains, both in dicots and monocots, always contain a downstream RRM domain (Fig. S8). The results here show that the fusion between the twin RIP domains and the RRM predates the monocot/dicot split and strongly suggest that the ancestral gene was involved in RNA editing.

Among the 11 RIP motif-containing proteins found in *Arabidopsis*, ORRM1 is the only member that has a known domain in addition to the RIP motif. The RRM domain present at the C terminus of ORRM1 is one of the most common protein domains in eukaryotes, and its involvement has been demonstrated in many posttranscriptional events, such as pre-mRNA processing, splicing, mRNA stability, and RNA editing (21). The mammalian apobec-1 complementation factor (ACF1) contains three RRM domains; with apobec-1, which carries the cytidine deaminase activity, ACF1 constitutes the minimal editosome needed for editing of *apo-B* mRNA in vitro (39). ACF binds to the *apo-B* mRNA in vitro and in vivo and is thought to attach to the mooring sequence of *apo-B* mRNA and to dock apobec-1 to deaminate its target cytidine (39). Although an RRM-containing protein is involved in mammalian editing, the function of ACF1 is most analogous to the PPR proteins' C target-recognition role in plant editing.

Complementation of the editing defect in the *orrm1* mutant by the sole RRM domain of ORRM1 was an unexpected observation. We speculate that the rescue of the editing defect by the RRM domain at a number of sites when protoplasts are transfected may be a result of the high level of expression often achieved during transient expression. The RNA binding studies (Fig. 8 and Fig. S7) indicate that the ORRM1 RRM exhibits at least some specificity for particular RNA sequences. In wild-type organelles, perhaps interaction of the RIP domains with PPR proteins plays a role in bringing the RRM domain in close proximity to the relevant RNA sequence.

In addition to ORRM1, another RRM-containing protein named CP31 has been implicated in plastid editing. CP31 belongs to a small family of 10 chloroplast ribonucleoproteins, all of which contain a twin RRM and an acidic amino-terminal domain (40, 41), but are in a different clade than ORRM1 (Fig. 3). CP31 was reported by Hirose and Sugiura (42) to be a common factor for editing of *psbL* and *ndhB* mRNAs in vitro. Immunodepletion of CP31 from the editing extract resulted in the inhibition of editing of *psbL* and *ndhB* mRNAs. More recently, a null mutant of *CP31A*, one of the two paralogues found in *Arabidopsis*, was shown to exhibit multiple specific editing defects in chloroplast transcripts (43). However, Tillich et al. (43) also observed that CP31 was responsible for the stability of specific chloroplast mRNAs, because almost no *ndhF* mRNA could be detected, and other chloroplast mRNAs were also depleted in *cp31a* mutants. In contrast, no transcripts were reduced in amount in *orrm1* (Table S1). The editing defect in *cp31a* mutant and the *cp31a*/*cp31b* double mutant is much less severe than ones that we observed in the *orrm1* mutant; an edited peak was detectable in the electrophoretograms of RT-PCR bulk sequences surrounding the editing sites most affected in *cp31a*/*cp31b* mutant (figure S2 in ref. 43). Bulk sequencing is a much less sensitive editing assay than either RNA-seq or PPE. If we had chosen bulk sequencing to assay the editing extent in the *orrm1* mutant plant, there would not have seen any detectable edited peak for the 12 sites whose editing extent in the *orrm1* mutant is < 0.1 (Table S1). Recently, Kupsch et al. (44) found that CP31A associates with large transcript pools and confers cold stress tolerance by influencing multiple chloroplast RNA processing events (44). The authors indicate that relative to its effect on RNA stability, the effect of CP31A on editing extent is minor.

The RRM domain of ORRM1 is most related to RRMs found in GR-RBPs and mRBPs, as well as RRMs found in a group referred to as S-RBPs (Fig. 2) (23). GR-RBPs have been shown to be involved in the plant's response to environmental stresses, particularly cold (45, 46). However, little is known about the molecular function of either GR-RBPs or mRBPs. Recently a rice GR-RBP protein named GRP162, which is likely orthologous to either *Arabidopsis* GR-RBP7 or GR-RBP8, was shown to be part of a restoration of fertility complex (47). GRP162 interacts in vivo with RF5, a PPR protein encoded by the fertility restorer gene *Rf5* to the Hong-Lian cytoplasmic male sterility. GRP162 was also shown to bind in vitro and in vivo to *atp6-orfH79*, the cytoplasmic male sterility-associated transcript (47), which is cleaved in the fertility-restored line. Like GRP162, ORRM1 interacts with a PPR protein and can bind to a transcript targeted for editing.

ORRM1 is the only well-characterized member of the ORRM clade of *Arabidopsis* proteins (Fig. 3). Among the 15 proteins whose RRM domains are most similar to the one found in ORRM1, there are seven GR-RBPs, eight mRBPs, and six S-RBPs (Table S3). There is overlap of the annotated mRBPs with both GR-RBPs and S-RBPs. Ten of these proteins are predicted to be targeted to either the plastid or the mitochondrion by both Predotar and TargetP, two prediction programs for subcellular localization of proteins (Table S3) (48, 49). Five of these proteins, which have a strong in silico prediction for organelle targeting, were found in the respective organelle by proteome MS/MS analysis (Table S3). None of these proteins have known functions except for the ribosomal protein RPS19. The ORRM subfamily of RRM proteins are obvious targets for further analysis to determine whether other family members are involved in plastid or mitochondrial editing.

Materials and Methods

Plant Material. The *Arabidopsis* T-DNA insertion line SALK_072648 was obtained from the *Arabidopsis* Biological Resource Center stock center. The wild-type plants come from several segregating T-DNA populations, all in the Col-0 background, which is similar to SALK_072648. WiscDsLox419C10 provided the wild-type plant for the total plastid RNA-seq and SAIL156A04, SAIL731D08, SALK016801, SALK114438, and GK-109E12 provided the wild-type plants for the gene specific RNA-seq, wt-1, wt-2, wt-3, wt-4, and wt-5, respectively. Plants were grown in 14 h of light/10 h of dark under full-spectrum fluorescent lights in a growth room at 26 °C. Genotyping was done by PCR with Qiagen Taq PCR master mix and primers listed in Table S4. Bulk-sequencing of the PCR product specific for the T-DNA insertion was done at Cornell University Life Sciences Core Laboratories Center.

The Zm-*orrm1-1* mutant was originally detected during the profiling of pigment and protein defects in maize mutants in the Photosynthetic Mutant Library (50) (http://pml.uoregon.edu/photosyntheticml.html): homozygous mutants were pale green and seedling-lethal, with strongly reduced levels of

photosystem I and cytochrome b6f proteins, and modest losses of Rubisco, ATP Synthase, and photosystem II proteins. An Illumina-based method (25) was used to identify *Mu* insertions that cosegregate with the mutant phenotype. An insertion in gene GRMZM5G899787 emerged from this analysis as the best candidate for the causal mutation because of the exonic location of the insertion and the fact that the gene encodes a predicted chloroplast protein related to proteins known to be involved in chloroplast gene expression. A second allele was identified during the large-scale sequencing of *Mu* insertions in each mutant in the PML collection. Complementation crosses between plants heterozygous for the two alleles yielded chlorophyll-deficient progeny whose protein deficiencies were similar to those in the parental alleles (Fig. 6), confirming that these defects result from disruption of GRMZM5G899787. GRMZM5G899787 is predicted to be the ortholog of *ORRM1* (At3g20930) by two independent ortholog prediction algorithms: OrthoMCL used at the Rice Genome Annotation Project (http://rice.plantbiology.msu.edu/), and the Ensembl pipeline used at Gramene (http://www.gramene.org). Protein extraction, RNA extraction, and immunoblotting were performed as described previously (51).

Phylogenetic Analysis. Protein alignments were achieved by using ClustalX 2.1 (52) and adjusted manually. The construction of phylogenetic trees was performed with MEGA5 (53). The presented tree was inferred using the Neighbor-Joining method (54) and evolutionary distances were computed using the Poisson-correction method. All positions containing alignment gaps and missing data were eliminated only in pair-wise sequence comparisons. Trees were also constructed using the UPGMA, maximum likelihood, maximum-parsimony, and minimum-evolution methods available on the MEGA5 software. One-thousand bootstrap replications were performed to determine the confidence level of the phylogenetic tree topology. Only representative of RRMs were used to construct the tree to avoid over-representation of certain groups, which would change the tree artificially.

Measure of Editing Extent. RNA extraction and RT-PCR methods were as previously described (4) and chloroplast isolation as described in Hayes and Hanson (55). Primers to amplify the mitochondrial and plastid transcripts have been previously described (4, 29, 56). Analysis of RNA editing by PPE was done as in ref. 29. The editing extent in maize plastid genes was measured primarily by bulk-sequencing of RT-PCR products amplified with primers listed in Table S4.

Measure of editing extent by RNA-seq was done by sequencing two kinds of templates, either cDNAs corresponding to organelle gene transcripts and amplified with organelle gene-specific primers, or cDNAs corresponding to the whole plastid transcriptome and reverse-transcribed with random hexamers. Gene-specific organelle cDNAs were quantified, mixed in equimolar ratio, and sheared by sonication; the sheared cDNA entered the workflow of low-throughput protocol for TruSeq RNA Sample Preparation Guide at the step of performing end repair. cDNAs corresponding to the whole plastid transcriptome were obtained by using total RNA prepared from plastid purified fraction on a percoll gradient (55); the RNA entered the workflow of low-throughput protocol for TruSeq RNA Sample Preparation Guide at the step of "elute, fragment, prime" RNA.

In the analysis, we used postfilter (PF) Illumina reads. After trimming the low-quality bases from both ends using the default settings of the seqtk trimfq program (https://github.com/lh3/seqtk), the resulting reads were aligned to the National Center for Biotechnology Information *Arabidopsis thaliana* chloroplast genomic template (NC_000932) using the TopHat program (57) with the default settings of two mismatches allowed per read. The C-to-T editing sites were determined using a combination of the programs samtools (58) and bedtools (59) and excel spreadsheets. The criteria were as follows: (*i*) the reference allele was C; (*ii*) the two major alleles were C and T; (*iii*) the sum of all alleles' depth (if any) was at most 20% of the depth of the second major allele; (*iv*) total C+T read depth was at least 20; and (*v*) the T fraction [T fraction = T/(C+T)] was $\geq$ 5%.

RNA Blots. RNA gel blot analysis was performed as described in Germain et al. (60). Primers used to make the probes are shown in Table S4.

Constructs Used in this Study. All of the primers are listed in Table S4.
Complementation constructs. ORRM1_1F_CACC and ORRM1_822R were used to amplify the N-terminal *ORRM1*, followed by TOPO cloning into pENTR/SD/D vector (Invitrogen). RecA _1F_CACC, RecA_ORRM1-C, ORRM1_823F, ORRM1_R were used in an overlapping PCR to amplify *ORRM1* C terminus fused with a RecA transit peptide sequence, followed by TOPO cloning into pENTR/SD/D vector. ORRM1_1F and ORRM1_R were used to amplify the full-length *ORRM1* coding sequence with the stop codon. These vectors were used in LR Clonase II recombination reactions with pEXSG-EYFP (61) to generate the full-length, N-terminal, and C-terminal *ORRM1* constructs driven by a 35S promoter.
Maize ORRM1 complementation constructs. Maize cDNA clone Zm_BFb0091M02 was obtained from the Maize Full Length cDNA Project. BP reaction was performed using pDONR201 (Invitrogen) and the cDNA clone, followed by LR reaction with pEXSG-EYFP (61) to clone the cDNA under the CaMV 35S promoter.
Y2H assay constructs. Coding sequences of mature PPR proteins and full-length, N-terminus, or C-terminus encoding portions of *ORRM1* were amplified with, respectively, and cloned into the PCR8/TOPO/GW vector. These sequences were then shuttled into the pGADT7GW and pGBKT7GW vectors (62) to create GAL4 activation domain (AD) fusion and DNA binding domain (BD) fusion, respectively.
Protein expression constructs. The mature *ORRM1* coding sequence was cloned by PCR using ORRM1_163F_BamHI and ORRM1_R_SalI. The PCR product was cloned into the pMal-TEV vector (63) using restriction digestion and ligation.

Y2H Assay. Two different mating types, α and a, of yeast stain PJ69-4 were used for transformation. The transformation procedures were performed following the original report (64). SD-leu-trp-his amino acid dropout media (Sunrise Science) were used to test the interaction. Yeast harboring both bait and prey constructs grown in liquid culture were diluted with sterile water to cell density 1×10^6, 1×10^5 cells/mL before spotting onto the plates. The picture of the growth was taken 3 d later. Each Y2H construct was paired with either AD or BD empty vector to test autoactivation in yeast using the same method with interaction assay. No autoactivation of HIS3 reporter was observed for the constructs used in this report.

Protoplast Transfection. These assays were performed as previously described (19).

Expression and Purification of Recombinant ORRM1. MBP-ORRM1 was expressed in *Escherichia coli* from the pMal-TEV vector, enriched by amylose affinity chromatography and further purified by gel-filtration chromatography using the method described previously for MBP-APO1 (51). The purity of the final preparation is illustrated in Fig. S7.

RNA Binding Assays. Synthetic RNAs (Integrated DNA Technologies) were 5′-end–labeled with [γ-32P]–ATP and T4 polynucleotide kinase, and purified on denaturing polyacrylamide gels. RNA binding reactions contained 100 mM NaCl, 40 mM Tris•HCl pH 7.5, 4 mM DTT, 0.1 mg/mL BSA, 0.5 mg/mL heparin, 10% glycerol (vol/vol), 10 units RNAsin (Promega), RNAs were at 15 pM and recombinant protein was at the following concentrations: 0, 125, 250, and 500 nM. Reactions were incubated for 20 min at 25 °C and resolved on 5% (wt/vol) native polyacrylamide gels. Results were visualized on a Storm phosphorimager. Data quantification was performed with ImageQuant (Molecular Dynamics).

ACKNOWLEDGMENTS. We thank Lin Lin for excellent technical assistance, especially with protein expression in *Escherichia coli*; Margarita Rojas (University of Oregon) for performing the RNA binding experiments; and Rosalind Williams-Carrier and Susan Belcher (University of Oregon) for identifying the Zm-*orrm1* mutants. This work was supported by the National Science Foundation from the Molecular and Cellular Biosciences, Gene and Genome Systems, Grants MCB-1020636 (to S.B.) and MCB-0929423 (to M.R.H.); National Science Foundation Grant IOS-0922560 (to A.B.); and a European Molecular Biology Organization Long-Term fellowship (to K.H.)

1. Gott JM, Emeson RB (2000) Functions and mechanisms of RNA editing. *Annu Rev Genet* 34:499–531.
2. Chateigner-Boutin AL, Small I (2007) A rapid high-throughput method for the detection and quantification of RNA editing based on high-resolution melting of amplicons. *Nucleic Acids Res* 35(17):e114.
3. Giegé P, Brennicke A (1999) RNA editing in *Arabidopsis* mitochondria effects 441 C to U changes in ORFs. *Proc Natl Acad Sci USA* 96(26):15324–15329.
4. Bentolila S, Elliott LE, Hanson MR (2008) Genetic architecture of mitochondrial editing in *Arabidopsis thaliana*. *Genetics* 178(3):1693–1708.
5. Gray MW, Covello PS (1993) RNA editing in plant mitochondria and chloroplasts. *FASEB J* 7(1):64–71.
6. Chateigner-Boutin AL, et al. (2008) CLB19, a pentatricopeptide repeat protein required for editing of *rpoA* and *clpP* chloroplast transcripts. *Plant J* 56(4):590–602.

7. Covello PS, Gray MW (1989) RNA editing in plant mitochondria. *Nature* 341(6243): 662–666.
8. Gualberto JM, Lamattina L, Bonnard G, Weil JH, Grienenberger JM (1989) RNA editing in wheat mitochondria results in the conservation of protein sequences. *Nature* 341(6243):660–662.
9. Hiesel R, Wissinger B, Schuster W, Brennicke A (1989) RNA editing in plant mitochondria. *Science* 246(4937):1632–1634.
10. Bock R, Hermann M, Kössel H (1996) In vivo dissection of *cis*-acting determinants for plastid RNA editing. *EMBO J* 15(18):5052–5059.
11. Choury D, Farré JC, Jordana X, Araya A (2004) Different patterns in the recognition of editing sites in plant mitochondria. *Nucleic Acids Res* 32(21):6397–6406.
12. Miyamoto T, Obokata J, Sugiura M (2002) Recognition of RNA editing sites is directed by unique proteins in chloroplasts: biochemical identification of *cis*-acting elements and *trans*-acting factors involved in RNA editing in tobacco and pea chloroplasts. *Mol Cell Biol* 22(19):6726–6734.
13. Hayes ML, Hanson MR (2007) Identification of a sequence motif critical for editing of a tobacco chloroplast transcript. *RNA* 13(2):281–288.
14. Lurin C, et al. (2004) Genome-wide analysis of *Arabidopsis* pentatricopeptide repeat proteins reveals their essential role in organelle biogenesis. *Plant Cell* 16(8):2089–2103.
15. Salone V, et al. (2007) A hypothesis on the identification of the editing enzyme in plant organelles. *FEBS Lett* 581(22):4132–4138.
16. Okuda K, et al. (2009) Pentatricopeptide repeat proteins with the DYW motif have distinct molecular functions in RNA editing and RNA cleavage in *Arabidopsis* chloroplasts. *Plant Cell* 21(1):146–156.
17. Okuda K, et al. (2010) The pentatricopeptide repeat protein OTP82 is required for RNA editing of plastid *ndhB* and *ndhG* transcripts. *Plant J* 61(2):339–349.
18. Zehrmann A, Verbitskiy D, Härtel B, Brennicke A, Takenaka M (2011) PPR proteins network as site-specific RNA editing factors in plant organelles. *RNA Biol* 8(1):67–70.
19. Bentolila S, et al. (2012) RIP1, a member of an *Arabidopsis* protein family, interacts with the protein RARE1 and broadly affects RNA editing. *Proc Natl Acad Sci USA* 109(22):E1453–E1461.
20. Takenaka M, et al. (2012) Multiple organellar RNA editing factor (MORF) family proteins are required for RNA editing in mitochondria and plastids of plants. *Proc Natl Acad Sci USA* 109(13):5104–5109.
21. Maris C, Dominguez C, Allain FH (2005) The RNA recognition motif, a plastic RNA-binding platform to regulate post-transcriptional gene expression. *FEBS J* 272(9): 2118–2131.
22. Bailey TL, et al. (2009) MEME SUITE: Tools for motif discovery and searching. *Nucleic Acids Res* 37(Web Server issue): W202-8.
23. Lorković ZJ, Barta A (2002) Genome analysis: RNA recognition motif (RRM) and K homology (KH) domain RNA-binding proteins from the flowering plant *Arabidopsis thaliana*. *Nucleic Acids Res* 30(3):623–635.
24. Vermel M, et al. (2002) A family of RRM-type RNA-binding proteins specific to plant mitochondria. *Proc Natl Acad Sci USA* 99(9):5866–5871.
25. Williams-Carrier R, et al. (2010) Use of Illumina sequencing to identify transposon insertions underlying mutant phenotypes in high-copy Mutator lines of maize. *Plant J* 63(1):167–177.
26. Zito F, Kuras R, Choquet Y, Kössel H, Wollman FA (1997) Mutations of cytochrome b6 in *Chlamydomonas reinhardtii* disclose the functional significance for a proline to leucine conversion by petB editing in maize and tobacco. *Plant Mol Biol* 33(1):79–86.
27. Boudreau E, Takahashi Y, Lemieux C, Turmel M, Rochaix JD (1997) The chloroplast *ycf3* and *ycf4* open reading frames of *Chlamydomonas reinhardtii* are required for the accumulation of the photosystem I complex. *EMBO J* 16(20):6095–6104.
28. Ruf S, Kössel H, Bock R (1997) Targeted inactivation of a tobacco intron-containing open reading frame reveals a novel chloroplast-encoded photosystem I-related gene. *J Cell Biol* 139(1):95–102.
29. Robbins JC, Heller WP, Hanson MR (2009) A comparative genomics approach identifies a PPR-DYW protein that is essential for C-to-U editing of the *Arabidopsis* chloroplast *accD* transcript. *RNA* 15(6):1142–1153.
30. Hammani K, et al. (2009) A study of new *Arabidopsis* chloroplast RNA editing mutants reveals general features of editing factors and their target sites. *Plant Cell* 21(11): 3686–3699.
31. Lu B, Hanson MR (1992) A single nuclear gene specifies the abundance and extent of RNA editing of a plant mitochondrial transcript. *Nucleic Acids Res* 20(21):5699–5703.
32. Chateigner-Boutin AL, Hanson MR (2002) Cross-competition in transgenic chloroplasts expressing single editing sites reveals shared *cis* elements. *Mol Cell Biol* 22(24): 8448–8456.
33. Hayes ML, Reed ML, Hegeman CE, Hanson MR (2006) Sequence elements critical for efficient RNA editing of a tobacco chloroplast transcript in vivo and in vitro. *Nucleic Acids Res* 34(13):3742–3754.
34. Neuwirt J, Takenaka M, van der Merwe JA, Brennicke A (2005) An in vitro RNA editing system from cauliflower mitochondria: editing site recognition parameters can vary in different plant species. *RNA* 11(10):1563–1570.
35. Okuda K, Nakamura T, Sugita M, Shimizu T, Shikanai T (2006) A pentatricopeptide repeat protein is a site recognition factor in chloroplast RNA editing. *J Biol Chem* 281(49):37661–37667.
36. Hammani K, et al. (2011) The pentatricopeptide repeat protein OTP87 is essential for RNA editing of *nad7* and *atp1* transcripts in *Arabidopsis* mitochondria. *J Biol Chem* 286(24):21361–21371.
37. Tasaki E, Hattori M, Sugita M (2010) The moss pentatricopeptide repeat protein with a DYW domain is responsible for RNA editing of mitochondrial *ccmFc* transcript. *Plant J* 62(4):560–570.
38. Alba MM, Pages M (1998) Plant proteins containing the RNA recognition motif. *Trends Plant Sci* 3(1):15–21.
39. Mehta A, Kinter MT, Sherman NE, Driscoll DM (2000) Molecular cloning of apobec-1 complementation factor, a novel RNA-binding protein involved in the editing of apolipoprotein B mRNA. *Mol Cell Biol* 20(5):1846–1854.
40. Ye LH, et al. (1991) Diversity of a ribonucleoprotein family in tobacco chloroplasts: Two new chloroplast ribonucleoproteins and a phylogenetic tree of ten chloroplast RNA-binding domains. *Nucleic Acids Res* 19(23):6485–6490.
41. Ruwe H, Kupsch C, Teubner M, Schmitz-Linneweber C (2011) The RNA-recognition motif in chloroplasts. *J Plant Physiol* 168(12):1361–1371.
42. Hirose T, Sugiura M (2001) Involvement of a site-specific trans-acting factor and a common RNA-binding protein in the editing of chloroplast mRNAs: Development of a chloroplast *in vitro* RNA editing system. *EMBO J* 20(5):1144–1152.
43. Tillich M, et al. (2009) Chloroplast ribonucleoprotein CP31A is required for editing and stability of specific chloroplast mRNAs. *Proc Natl Acad Sci USA* 106(14):6002–6007.
44. Kupsch C, et al. (2012) Arabidopsis chloroplast RNA binding proteins CP31A and CP29A associate with large transcript pools and confer cold stress tolerance by influencing multiple chloroplast RNA processing steps. *Plant Cell* 24(10):4266–4280.
45. Kim YO, Kim JS, Kang H (2005) Cold-inducible zinc finger-containing glycine-rich RNA-binding protein contributes to the enhancement of freezing tolerance in *Arabidopsis thaliana*. *Plant J* 42(6):890–900.
46. Kim JS, et al. (2007) Cold shock domain proteins and glycine-rich RNA-binding proteins from *Arabidopsis thaliana* can promote the cold adaptation process in *Escherichia coli*. *Nucleic Acids Res* 35(2):506–516.
47. Hu J, et al. (2012) The rice pentatricopeptide repeat protein RF5 restores fertility in Hong-Lian cytoplasmic male-sterile lines via a complex with the glycine-rich protein GRP162. *Plant Cell* 24(1):109–122.
48. Small I, Peeters N, Legeai F, Lurin C (2004) Predotar: A tool for rapidly screening proteomes for N-terminal targeting sequences. *Proteomics* 4(6):1581–1590.
49. Emanuelsson O, Nielsen H, Brunak S, von Heijne G (2000) Predicting subcellular localization of proteins based on their N-terminal amino acid sequence. *J Mol Biol* 300(4):1005–1016.
50. Stern DB, Hanson MR, Barkan A (2004) Genetics and genomics of chloroplast biogenesis: Maize as a model system. *Trends Plant Sci* 9(6):293–301.
51. Watkins KP, et al. (2011) APO1 promotes the splicing of chloroplast group II introns and harbors a plant-specific zinc-dependent RNA binding domain. *Plant Cell* 23(3): 1082–1092.
52. Thompson JD, Gibson TJ, Plewniak F, Jeanmougin F, Higgins DG (1997) The CLUSTAL_X windows interface: Flexible strategies for multiple sequence alignment aided by quality analysis tools. *Nucleic Acids Res* 25(24):4876–4882.
53. Tamura K, et al. (2011) MEGA5: Molecular evolutionary genetics analysis using maximum likelihood, evolutionary distance, and maximum parsimony methods. *Mol Biol Evol* 28(10):2731–2739.
54. Saitou N, Nei M (1987) The neighbor-joining method: A new method for reconstructing phylogenetic trees. *Mol Biol Evol* 4(4):406–425.
55. Hayes ML, Hanson MR (2007) Assay of editing of exogenous RNAs in chloroplast extracts of *Arabidopsis*, maize, pea, and tobacco. *Methods Enzymol* 424:459–482.
56. Bentolila S, Knight WE, Hanson MR (2010) Natural variation in *Arabidopsis* leads to the identification of REME1, a pentatricopeptide repeat-DYW protein controlling the editing of mitochondrial transcripts. *Plant Physiol* 154(4):1966–1982.
57. Trapnell C, Pachter L, Salzberg SL (2009) TopHat: Discovering splice junctions with RNA-Seq. *Bioinformatics* 25(9):1105–1111.
58. Li H, et al.; 1000 Genome Project Data Processing Subgroup (2009) The sequence alignment/map format and SAMtools. *Bioinformatics* 25(16):2078–2079.
59. Quinlan AR, Hall IM (2010) BEDTools: A flexible suite of utilities for comparing genomic features. *Bioinformatics* 26(6):841–842.
60. Germain A, et al. (2011) Mutational analysis of *Arabidopsis* chloroplast polynucleotide phosphorylase reveals roles for both RNase PH core domains in polyadenylation, RNA 3′-end maturation and intron degradation. *Plant J* 67(3):381–394.
61. Jakoby MJ, et al. (2006) Analysis of the subcellular localization, function, and proteolytic control of the *Arabidopsis* cyclin-dependent kinase inhibitor ICK1/KRP1. *Plant Physiol* 141(4):1293–1305.
62. Horák J, et al. (2008) The *Arabidopsis thaliana* response regulator ARR22 is a putative AHP phospho-histidine phosphatase expressed in the chalaza of developing seeds. *BMC Plant Biol* 8:77.
63. Williams-Carrier R, Kroeger T, Barkan A (2008) Sequence-specific binding of a chloroplast pentatricopeptide repeat protein to its native group II intron ligand. *RNA* 14(9):1930–1941.
64. Gietz RD, Schiestl RH, Willems AR, Woods RA (1995) Studies on the transformation of intact yeast cells by the LiAc/SS-DNA/PEG procedure. *Yeast* 11(4):355–360.
65. Barkan A (1993) Nuclear mutants of maize with defects in chloroplast polysome assembly have altered chloroplast RNA metabolism. *Plant Cell* 5(4):389–402.
66. Kroeger TS, Watkins KP, Friso G, van Wijk KJ, Barkan A (2009) A plant-specific RNA-binding domain revealed through analysis of chloroplast group II intron splicing. *Proc Natl Acad Sci USA* 106(11):4537–4542.